Open Access Library Journal
2026, Volume 13, e15776
ISSN Online: 2333-9721
ISSN Print: 2333-9705

Assessment of Indoor Radon Concentration and Its Health Impacts: Insights from a Mountainous Region

Mavia Anjum[1*], Ahmed Hashir[2], Simab Jamil[2], Ayesha Khalid[2], Mustansar Nadeem[2], Muhammadhu Ameen Muhammadhu Azmin[3], Mathar Bashir[4], Ansar Abbas[3], Hannan Younis[3]

[1]Department of Physics, University of Idaho, Moscow, USA
[2]Department of Physics, Federal Urdu University of Arts, Science & Technology (FUUAST), Islamabad, Pakistan
[3]Radiation Physics Lab, Department of Physics, COMSATS University Islamabad, Islamabad, Pakistan
[4]Department of Chemistry, University of Idaho, Moscow, USA
Email: *mav.mavia14@gmail.com

How to cite this paper: Anjum, M., Hashir, A., Jamil, S., Khalid, A., Nadeem, M., Azmin, M.A.M., Bashir, M., Abbas, A. and Younis, H. (2026) Assessment of Indoor Radon Concentration and Its Health Impacts: Insights from a Mountainous Region. *Open Access Library Journal*, **13**: e15776.
https://doi.org/10.4236/oalib.1115744

Received: July 17, 2026
Accepted: August 24, 2026
Published: August 27, 2026

Abstract

Radon is a naturally occurring radioactive gas produced by uranium decay in soil and rocks, and the dominant source of natural ionizing radiation exposure. Prolonged indoor inhalation of its alpha-emitting progeny is the second leading cause of lung cancer after tobacco smoking. This study provides the assessment of indoor radon concentrations in 25 dwellings across five villages in a mountainous region in northern Pakistan. These villages (Kamra, Thoon, Paija, Bhattian, and Chaffar) are in Kotli Sattian, a seismically active sub-Himalayan township in Rawalpindi District, Punjab, Pakistan. The CR-39 solid-state nuclear track detectors were used passively at head height for 60 days for track counting. The overall mean radon concentration was 43.75 ± 31.04 $Bq \cdot m^{-3}$, ranging from 13.77 to 135.76 $Bq \cdot m^{-3}$. Village-level means ranged from 33.10 $Bq \cdot m^{-3}$ (Bhattian) to 51.85 $Bq \cdot m^{-3}$ (Chaffar). Newly constructed concrete and brick dwellings recorded a higher mean (49.44 $Bq \cdot m^{-3}$) than older mud and wood structures (35.42 $Bq \cdot m^{-3}$), attributable to the elevated radium content of modern building materials. The mean annual effective dose of 0.11 $mSv \cdot y^{-1}$ is well below the 1 $mSv \cdot y^{-1}$ public limit. The Excess Lifetime Cancer Risk (ELCR) of 0.37×10^{-3} and Lung Cancer Risk (LCR) of 5.07×10^{-3} both fall within internationally accepted limits. These findings establish a radiological baseline for Kotli Sattian and highlight the need for year-round monitoring and targeted remediation in dwellings proximal to active fault structures.

Subject Areas

Geology, Nuclear Physics

Keywords

Indoor Radon, Nuclear Track Detectors, Annual Effective Dose, Dosimetry, Health Risk Assessment

1. Introduction

The existence of ionizing radiation from natural sources is an intrinsic aspect of life on Earth, persistently impacting human beings and an unavoidable characteristic of life on our planet [1]. The presence of radon and its rapidly decaying by-products in the atmosphere is the primary source of human exposure to naturally occurring ionizing radiation. Radon is a naturally occurring radioactive gas that is part of the decay series of Uranium. It is found naturally in soil, water and rocks in varying amounts [2] [3]. The levels of uranium on Earth exhibit variation due to the varying concentrations of uranium in different types of rocks and soils, such as granite, uranium-enriched phosphatic rocks, and shale [4] [5]. The concentration of radon in outdoor air is often low. However, if it is unable to dissipate, it might accumulate to higher concentration levels in the indoor environment [6]. Indoor radon primarily originates from soil and building materials, such as sand, pebbles, and cement, that contain trace levels of U-238. Radon may penetrate indoor environments through the ground in regions with high seismic activity [7] [8].

The World Health Organization (WHO) has recognized radon as being one of the 19 ecological toxins. Radon is the 2nd primary contributor to lung tumors, trailing the use of tobacco products, as per the U.S. Environmental Protection Agency (EPA). It is a major cause of lung cancer in nonsmokers [9]. Radon causes an estimated 3% to 14% of lung cancer cases, depending on the average level of radon in country and the smoking prevalence [10] [11]. Countries and organizations advise restricting indoor radon levels to minimize health hazards. The International Commission on Radiological Protection (ICRP) recommends implementing preventive measures when the radon concentration in residential areas exceeds 300 $Bq \cdot m^{-3}$ and in occupational settings surpasses 1000 $Bq \cdot m^{-3}$ [12]. Long-term exposure to radon concentrations increases the risk of developing lung cancer by 16% for each 100 $Bq \cdot m^{-3}$ increment [12].

Human beings could be exposed to artificial radiation in modern times, specifically from medical procedures [13] but the primary source of human exposure to natural ionizing radiation is predominantly radon [14]. The global radon contribution accounts for up to 50% of the total radiation dosage, with a value of around 1.15 $mSv \cdot y^{-1}$ [15]. During the process of radon decay, alpha radioactive particles are emitted and can be ingested and deposited on our bodies. Additionally, Alpha particles have the ability to disturb the DNA structure within the cells of the epithelial membrane, particularly in lung cells. Exposure to this type of radiation is known to significantly raise the likelihood of developing lung cancer [16]. The recommended indoor radon levels from various organizations are ICRP (300

Bq·m^{-3}), USEPA (150 Bq·m^{-3}), and WHO (100 - 300 Bq·m^{-3}) [12] [17] [18].

The concentration of Radon in a house is influenced by several factors, including the makeup of the underlying soil, the materials used in building construction (such as cement and sand), the ventilation, and the flow of air both inside and outside the building's walls [19]. Radon can infiltrate houses and buildings by multiple paths, such as fissures in floors and walls, openings around pipes, and even through well water. This can result in fluctuating indoor concentrations of radon [20]. Basements offer a substantial amount of exposed surface area that comes into contact with rock and soil materials. The concentration of Radon is typically elevated in basements of a dwelling [21].

The concentration of radon within a residence varies on a daily and hourly basis. To account for these variations, it is advisable to estimate the average annual concentration of radon in indoor air over a minimum duration of two months. The measurement of radon levels in houses can be done using either active [3] or passive nuclear techniques. However, the passive technique, which involves the use of Nuclear Track Detectors, is both cheaper and more convenient [22]. This method entails the placement of solid-state detectors (namely CR-39) in different rooms within homes. As Radon is an alpha emitter, the alpha rays produced during its decay pass through the detector and leave tracks. These tracks are used to measure the level of radon in an area. The CR-39 detectors are strategically positioned in a certain location to monitor the concentration of radon over a predetermined period, usually spanning many months [23].

Kotli Sattian is a town situated in the mountainous region of the northern Punjab province of Pakistan. The region experiences predominantly temperate climatic conditions and is situated near the Punjab and Kashmir borders. Most of the population resides in dwellings constructed from clay and wood, although there has been a recent trend towards modernization, with an increasing number of people opting to build concrete buildings. Because the region is in a seismically active zone, these houses are not well repaired and as a result, they have cracks and pores through which radon gas can penetrate and harm the inhabitants. This study aimed to evaluate the levels of indoor radon concentrations in the five villages of Kotli Sattian and investigate the health effects of radon exposure on the local population. To achieve this objective, CR-39 nuclear track detectors were carefully placed in 25 distinct residences. The CR-39 detectors were set up for a duration of 60 days, and subsequently, they underwent a process of etching in the Radiation Physics laboratory at COMSATS University Islamabad. This procedure allowed for the estimation of the radon concentration. The region is still in developing phase and lacks a thorough investigation of indoor radon concentration and its impact on health. This study attempts to fill this gap by providing a baseline for this region and establishing a foundation for future research.

2. Materials and Methods

2.1. Study Area

Kotli Sattian is a municipality located in the Rawalpindi District of Punjab, Pakistan. It is a subdivision of the Rawalpindi district. From a geographical perspective, it is surrounded on the east by the Jhelum River, on the southwest by the Soan River, and on the northwest by Murree [24]. In addition, Kotli Sattian is adjacent to Kahuta Tehsil to the south. Kotli Sattian is connected to the Kashmir Territory in the east via a bridge over the river Jhelum, as well as to the southwest. Moreover, it is located next to Islamabad. The maximum elevation is at Pofandi peak, located east of the Patriata spur, with an altitude above 7035 feet above sea level. The nadir is situated along the Jhelum River at Patton, at an elevation of 1587 feet relative to sea level. In seismically active regions, the geological setting plays a particularly amplifying role: fault zones serve as preferential pathways for radon migration due to their increased porosity and permeability [25], allowing radon to travel from deeper crustal sources toward the surface far more rapidly than diffusion through intact rock would permit [8]. Two main mechanisms of radon discharge from soil gas in active fault zones have been identified: diffusion and dispersion from permeable soil, and upwelling directly from fault planes, with higher concentrations and flux consistently observed at fault locations [26]. In the sub-Himalayan fold-and-thrust belt where Kotli Sattian is situated, the intersection of uranium-bearing metamorphic basement rocks and active seismic faults therefore represents a geologically favorable setting for elevated soil-gas radon, providing the fundamental geogenic context for the indoor concentrations measured in this study. Radon measurements were conducted in five villages, specifically Kamra, Bhattian, Paija, Thoon, and Chaffar. The study area map is given in **Figure 1** and the details of the houses are given in **Table 1**.

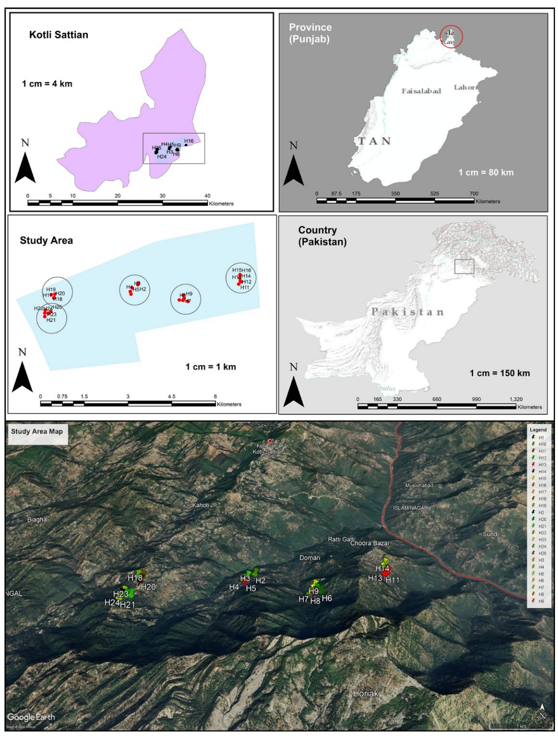

Figure 1. Study area map.

2.2. Selection of Houses

A total of twenty-five dwellings were chosen, and 5 dosimeters were carefully positioned in different spots within the houses across the five villages in the Kotli Sattian region. Five houses were chosen in every village as locations for dosimeter installation. Copper Wire was used to suspend the dosimeters at a height of 5 - 6 feet in each house. The houses in Bhattian, Paija, and Thoon were built using bricks, cement blocks, and concrete. The newly constructed dwellings for our inquiry were designated as these buildings. The houses in Chaffar and Kamra were categorized as old homes, built with mud and wood.

Table 1. Location details of houses selected for this study, Radon concentration and Annual Effective dose.

House ID	Latitude (Decimal Degrees)	Longitude (Decimal Degrees)	Village	Radon concentration ($Bq \cdot m^{-3}$)	Annual effective dose ($mSv \cdot y^{-1}$)
H1	33.7558	73.5231	Kamra	33.29	0.084
H2	33.7553	73.5230		23.28	0.059
H3	33.7543	73.5213		22.63	0.057
H4	33.7532	73.5207		25.33	0.064
H5	33.7524	73.5209		84.36	0.213
H6	33.7502	73.5384	Thoon	33.26	0.084
H7	33.7505	73.5369		24.10	0.061
H8	33.7506	73.5358		21.64	0.055
H9	33.7511	73.5373		37.88	0.096
H10	33.7521	73.5370		135.76	0.343
H11	33.7555	73.5541	Paija	69.60	0.176
H12	33.7565	73.5546		77.47	0.195
H13	33.7562	73.5549		22.14	0.056
H14	33.7574	73.5544		28.04	0.071
H15	33.7584	73.5545		30.25	0.076
H16	33.7583	73.5545	Bhattian	23.61	0.060
H17	33.7513	73.4972		33.20	0.084
H18	33.7522	73.4963		27.55	0.069
H19	33.7524	73.4974		28.78	0.073
H20	33.7512	73.4971		52.34	0.132
H21	33.7455	73.4943	Chaffar	30.01	0.076
H22	33.7466	73.4943		91.74	0.231
H23	33.7475	73.4945		13.77	0.035
H24	33.7465	73.4954		24.10	0.061
H25	33.7470	73.4962		99.61	0.251

2.3. Preparation of Radon Dosimeters

Radon dosimeters utilized for extended surveys must exhibit qualities such as small dimensions, cost-effectiveness, and ease of use. The sensitivity of a dosimeter depends on the choice of material, as well as the size and placement of the detector within the dosimeter. The dosimeter consists of a cylindrical plastic case with a radius of 3 cm and a height of 7.5 cm. These dosimeters have one side that is exposed, while the opposite side is sealed with a cap. The detector is affixed to the lid utilizing double-sided tape. The Radon dosimeters (Figure 2) were obtained and calibrated in the Radiation Physics Laboratory (RPL) at COMSATS University Islamabad.

Figure 2. Closed and open view of dosimeter that consists of a cylindrical plastic bottle with detector fixed below the lid of the dosimeter.

The CR-39 is attached to the dosimeter cap using double-sided tape, assuring its strong fixation. The dosimeter was enclosed in a plastic bag that efficiently resists moisture and blocks the entry of particles of dust from the surrounding air. The dosimeter was installed for a period of sixty days. The CR-39 nuclear track detector was used for radon measurements because of its exceptional sensitivity, resilience to various environmental factors, and superior visual clarity. The selection was made to use CR-39 sheets with an average thickness of 0.9mm due to their robustness and ability to avoid detection of any markings on the rear surface by the image analyzer. The CR-39 sheets were accurately partitioned into rectangular segments measuring 4 cm in length and 2.5 cm in width using a laser cutter. A unique serial number was engraved on each detector to aid in identification. View and specifications of CR-39 detector are shown in Figure 3. Figure 3(a) shows a view of CR-39 detector used in our study while Figure 3(b) shows a schematic view of the dosimeter. Radon concentration was calculated by applying the conversion factor of dosimeter as 0.012 tracks·cm^{-2}·h^{-1} is equal to 1 Bq·m^{-3}.

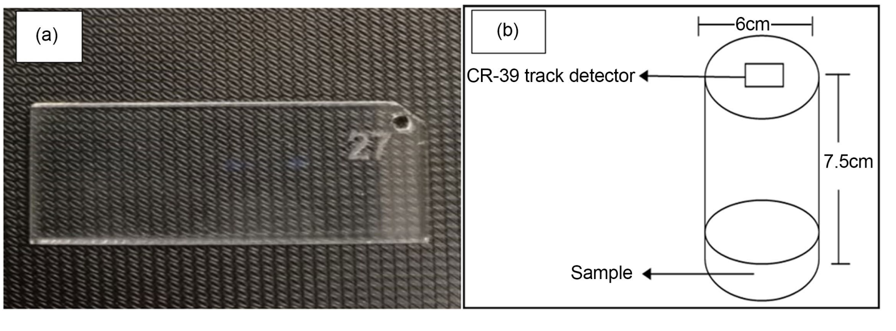

Figure 3. (a) A View of CR-39 detector; (b) A View of dosimeter for this study.

2.4. Dosimeter Collection and Etching

Dosimeters were set at head heights in five houses of each community in Kotli Sattian. After a duration of 60 days, the dosimeters were retrieved and carefully transported back to the laboratory without any contamination. The detectors were removed from the dosimeter to receive etching. The CR-39 detectors underwent etching in a 6-molar solution (6M) of NaOH at a temperature of 70˚C for a duration of three hours (Figure 4). Following the etching process, the CR-39 samples were removed from the solution, rinsed with pure water, and dried flat using tissue wipes to eliminate the etchant and etch products from the detector's surface.

2.5. Track Density and Radon Concentration Calculation

The average number of tracks accumulated during a 60-day period was determined by counting the average number of tracks in a CR-39 detector under x10 magnification, using 20 - 25 fields of view. The track density was calculated by multiplying the calibration of the microscope (×10) by the average number of tracks observed in each field of view. The track density per hour was determined by translating the exposure time into hours. The radon concentration was determined by utilizing the given equation.

$$\text{Radon Concentration}\left(\text{Bq}\cdot\text{m}^{-3}\right)=\frac{\text{Track Density}}{\text{Conversion Factor of the Dosimeter}} \quad (1)$$

The conversion factor of dosimeter used is 0.012 tracks·cm^{-2}·h^{-1}.

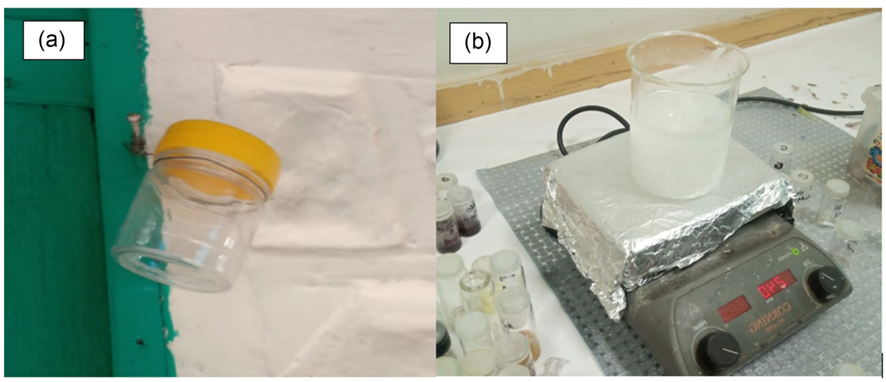

Figure 4. (a) Installed dosimeter in the house; (b) Etching of the Cr-39 detector for track counting.

3. Results and Discussion

The radon concentration for 25 houses was calculated, and the values are given in Table 1. The mean radon concentration in this study was found to be 43.75 ± 31.04 Bq·m^{-3}, ranging from 13.77 to 135.76 Bq·m^{-3}. The houses have radon activity below the standard value provided by the US-EPA, which is 150 Bq·m^{-3}. The indoor radon concentration was relatively high in six houses, specifically H5, H10, H11, H12, H22, and H25. The H10, H11 and H12 are the new concrete houses and the radon concentration in new houses is higher due to radioactive Ra-226 present in the construction materials in higher amounts [27]. Although mud and wood construction often results in reduced radon emission compared to cement and brick, three residences in Chaffar and Kamra (H5, H22, H25) demonstrated significantly heightened radon levels (84.36, 91.74, and 99.61 Bq/m^3, respectively). This is due to the interplay of the region's seismic activity with the structural integrity of older buildings. Faults and fractures operate as favorable conduits for radon gas migration from the lower crust to the surface, resulting in increased soil-gas radon levels in tectonically active regions [28]. Kotli Sattian is situated on the seismically active Muzaffarabad Fault in the NW Himalayas; radon concentrations along this fault exhibit a significant negative correlation with distance from the fault ($R^2 = 0.73$), with the highest concentrations observed closest to the fault zone [29]. Research on the Balakot-Bagh Fault in Northern Pakistan indicates that soil-gas radon concentrations are markedly higher near the fault (mean 11.9 kBq/m^3) than in nearby regions [30]. Radon-laden soil gas infiltrates structures via cracks and fissures in foundations due to pressure differentials, as indoor air pressure is generally lower than the pressure of the underlying soil gas [31]. In outdated mud and wood dwellings, fissures in floors and walls resulting from years of structural settlement and seismic micro-tremors act as direct conduits for the ingress of soil-gas radon [31]. Low-income households in rural mountainous Pakistan generally lack the means to repair and seal such entrance holes, resulting in the gradual accumulation of structural vulnerability. We emphasize that the kind of building material alone does not dictate indoor radon risk; the interplay of geological conditions, structural soundness, and socioeconomic ability for maintenance is equally vital. In terms of villages, the highest radon concentration was found in Chaffar *i.e.* 51.7 Bq·m^{-3} and lowest in Bhattian 33.3 Bq·m^{-3}. The average radon concentration in different villages of Kotli Sattian are given in **Table 2** alongside average track densities and annual effective doses. The average radon concentrations in five villages are also plotted using GIS tool Inverse Distance Weighting Interpolation (IDW) in **Figure 5**.

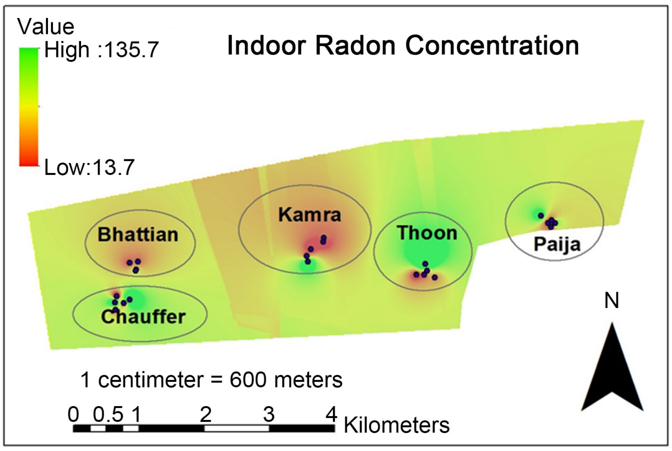

Figure 5. Spatial Distribution of Radon activity in different villages calculated using Inverse distance weighting interpolation (IDW).

3.1. Village-Level Radon Concentrations

The mean radon concentrations across the five villages, alongside average track densities and annual effective doses, are summarised in **Table 2**, and the spatial distribution of radon activity is illustrated through Inverse Distance Weighting (IDW) interpolation in **Figure 5**. At the village level, the highest mean radon concentration was recorded in Chaffar (51.85 ± 40.53 $Bq\cdot m^{-3}$), followed by Thoon (50.53 ± 48.10 $Bq\cdot m^{-3}$), Paija (45.50 ± 25.91 $Bq\cdot m^{-3}$), Kamra (37.78 ± 26.38 $Bq\cdot m^{-3}$), and the lowest in Bhattian (33.10 ± 11.29 $Bq\cdot m^{-3}$). The large standard deviations observed particularly in Chaffar (CV = 78.2%) and Thoon (CV = 95.2%) indicate substantial intra-village variability in radon concentrations. Indoor radon concentration can vary highly from place to place, and even from room to room within the same dwelling, as it is influenced by geological, building-related, meteorological, and socio-economic factors acting simultaneously [32] [33]. Among these contributors, geological factors are the most variable, while ventilation variation among houses is generally responsible for radon variations comparable to those introduced by building materials, and is more significant at lower ventilation rates. In Chaffar specifically, the wide range from 13.77 $Bq\cdot m^{-3}$ (H23) to 99.61 $Bq\cdot m^{-3}$ (H25) within the same village reflects the local heterogeneity of soil radon potential, which even within a relatively homogeneous area can exert a strong influence on indoor concentrations [34]. In contrast, Bhattian exhibited the lowest inter-house variability (CV = 34.1%), with values ranging narrowly from 23.61 to 52.34 $Bq\cdot m^{-3}$, suggesting a more homogeneous sub-surface radon source in that locality.

The elevated concentrations in Chaffar and Thoon, despite belonging to different construction categories (old mud/wood and new concrete respectively), point to geology as the dominant driver over building material type in these cases. The physical and chemical properties of soil, including porosity and permeability, significantly affect the migration and release of radon from underground sources into the indoor environment [34]. The presence of faults allows for the migration of radon gas from deeper geological origins, favouring its entry into homes; high radon emissions are more likely to be found in permeable soils such as sandy or gravelly soils, whereas fine soils act as a natural barrier to the upward movement of gas [34]. Kotli Sattian lies in a tectonically active zone of the sub-Himalayan fold-and-thrust belt, where permeable fractured geology facilitates vertical radon transport irrespective of surface construction type. Geological characteristics and meteorological parameters present synergistic effects on indoor radon levels, and indoor radon concentrations are reportedly more sensitive to meteorological parameters than to building characteristics alone [35] [36]. A review of 31 indoor radon studies from different countries revealed a weighted mean indoor radon concentration of 178 $Bq\cdot m^{-3}$ with a standard deviation of 193 $Bq\cdot m^{-3}$, underscoring the extent to which local geological and meteorological conditions drive variability between regions [36].

Table 2. Averages track densities, mean radon concentrations and annual effective doses in five villages of Kotli Sattian, Pakistan.

Village	Average Track Density per hour	Mean Radon Concentration ($Bq \cdot m^{-3}$)	Annual Effective Dose ($mSv \cdot y^{-1}$)
Chaffar	0.44	51.85 ± 40.53	0.13
Kamra	0.45	37.5 ± 26.38	0.10
Thoon	0.55	50.53 ± 48.10	0.13
Paija	0.61	45.50 ± 34.52	0.11
Bhattian	0.62	33.10 ± 33.00	0.08

3.2. Annual Effective Dose

In radiation protection, the annual effective dose is expressed in units of $mSv \cdot y^{-1}$ and is utilized to evaluate the quantity of radiation exposure and radionuclide intake for the public and workers. The following equation is employed to estimate the average annual effective dose of radon to the Kotli Sattian population that is caused by indoor radon:

$$H = C * F * O * T * D \tag{2}$$

The variables in the equation are as follows: H is the annual effective dose, C represents the indoor radon concentration in $Bq \cdot m^{-3}$, F is the adjustment factor with a value of 0.4 for indoor measurement, O is the occupancy factor with a value of 0.8 for indoor measurement, T represents the number of hours in a year 8784 $h \cdot y^{-1}$, and D is the dose conversion factor with a value of 0.9 $nSv \cdot Bq^{-1} \cdot m^{-3} \cdot h^{-1}$ (0.9) [22] [37].

Table 3 presents the annual effective dose for each individual residence. At the household level, the maximum annual effective dosage was observed in H10, Thoon (0.343 $mSv \cdot y^{-1}$), associated with the peak individual radon concentration of 135.76 $Bq \cdot m^{-3}$, whereas the minimum was noted in H23, Chaffar (0.035 $mSv \cdot y^{-1}$), linked to the lowest concentration of 13.77 $Bq \cdot m^{-3}$. The computed mean annual effective doses at the village level are shown in Table 2. The highest mean annual effective dosage was reported in Chaffar (0.13 $mSv \cdot y^{-1}$) and Thoon (0.13 $mSv \cdot y^{-1}$), followed by Paija (0.11 $mSv \cdot y^{-1}$) and Kamra (0.10 $mSv \cdot y^{-1}$), with the lowest observed in Bhattian (0.08 $mSv \cdot y^{-1}$). The mean yearly effective dosage for all 25 residences in Kotli Sattian was determined to be 0.11 $mSv \cdot y^{-1}$.

All annual effective dose levels documented in this study are below the recommended public exposure action level of 1 $mSv \cdot y^{-1}$, as specified by ICRP, US-EPA, and WHO, demonstrating that radon-related radiation exposure in Kotli Sattian remains within internationally recognized limits. This finding aligns with similar research conducted in Pakistan. A research in the Murree region, adjacent to the current study area, showed a mean annual effective dosage of 0.733 $mSv \cdot y^{-1}$ [38], exceeding our values, possibly due to the varying geological sub-zones within the larger Murree formation. Research in the Punjab Province of Pakistan indicated mean annual effective doses of 1.39 ± 0.78 $mSv \cdot y^{-1}$ [39], whereas significantly elevated values of 3.5 - 5.1 $mSv \cdot y^{-1}$ were observed in the Hazara Division [40], highlighting the impact of uranium-rich geology and diminished winter ventilation in those areas. In the sub-Himalayan area of Kotli, Azad Jammu and Kashmir, which possesses geological characteristics directly comparable to Kotli Sattian, the mean annual effective dosage was 1.8 mSv·y^{-1}, due to the uranium-bearing geological formations present in the region [32]. The relatively low doses in Kotli Sattian indicate that, despite the seismically active environment, the local geology does not yield uranium-rich rocks at a concentration adequate to generate harmful indoor radon levels under present conditions.

It is important to acknowledge that the dosage numbers presented are derived from a singular 60-day assessment window and do not account for seasonal fluctuations. Indoor radon levels are generally heightened during winter months owing to less ventilation and greater pressure differentials between indoor air and soil gas [32]. Future research should use year-round data to comprehensively characterize the annual dosage load on the population of Kotli Sattian.

3.3. Excess Lifetime Cancer Risk (ELCR)

The Excess Lifetime Cancer Risk (ELCR) measures the increased likelihood of getting terminal cancer during an individual's lifetime as a result of prolonged exposure to indoor radon. It is computed as:

$$\mathbf{ELCR} = \mathbf{E} \times \mathbf{DL} \times \mathbf{RF} \tag{3}$$

where **E** is the annual effective dose (mSv·y^{-1}); **DL** is the life expectancy of Pakistan = 67.1 years [41]; and **RF** is the ICRP fatal cancer risk coefficient = 5 × 10^{-5} mSv^{-1} (*i.e.* 0.05 Sv^{-1}) [42]. The calculated ELCR values for all five villages of Kotli Sattian are presented in Table 3. The overall mean ELCR across the study area was **0.3703 × 10^{-3}**. At the village level, the highest ELCR was recorded in Chaffar (0.4388 × 10^{-3}), followed by Thoon (0.4277 × 10^{-3}), Paija (0.3851 × 10^{-3}), Kamra (0.3198 × 10^{-3}), and the lowest in Bhattian (0.2801 × 10^{-3}). The ICRP Publication 103 [42] defines an acceptable ELCR range of **0.29 × 10^{-3} to 1.45 × 10^{-3}** for the general public from a single source. Four of the five villages (Kamra, Thoon, Paija, and Chaffar) fall within this range. Bhattian recorded an ELCR of 0.2801 × 10^{-3}, marginally below the lower bound, consistent with it having the lowest mean radon concentration in the study (33.10 Bq·m^{-3}). The overall mean ELCR of 0.3703 × 10^{-3} is well within the acceptable range, confirming that the population of Kotli Sattian does not face an elevated lifetime cancer risk from indoor radon under current conditions.

Table 3. Village-level radon concentration, annual effective dose, Excess Lifetime Cancer Risk (ELCR), and Lung Cancer Risk (LCR).

Village	Mean C (Bq·m^{-3})	E (mSv·y^{-1})	ELCR (×10^{-3})	LCR (×10^{-3})	ICRP ELCR and LCR Status
Kamra	37.78	0.0953	0.3198	4.3822	Within ✓
Thoon	50.53	0.1275	0.4277	5.8612	Within ✓
Paija	45.50	0.1148	0.3851	5.2780	Within ✓
Bhattian	33.10	0.0835	0.2801	3.8391	Low ✓
Chaffar	51.85	0.1308	0.4388	6.0141	Within ✓
Overall	**43.75**	**0.1104**	**0.3703**	**5.0750**	**Within ✓**

3.4. Lung Cancer Risk (LCR) from Indoor Radon

Radon exposure carries a specific, well-characterised risk for lung cancer the primary radiological health outcome of concern. The WHO estimates that radon accounts for 3% - 14% of all lung cancers nationally, depending on mean indoor radon concentration and smoking prevalence [18]. The radon-specific lung cancer risk (LCR) is calculated as:

$$\mathbf{LCR} = \mathbf{C} \times \mathbf{1.16} \times \mathbf{10}^{-4} \quad (4)$$

where **C** is the mean indoor radon concentration (Bq·m^{-3}), and 1.16×10^{-4} is the WHO lifetime lung cancer risk coefficient per unit radon concentration [18] [43].

The LCR values for all five villages are presented alongside the ELCR values in **Table 3**. The overall mean LCR was **5.075×10^{-3}** (approximately 507 cases per 100,000 persons). The highest village-level LCR was recorded in Chaffar (6.014×10^{-3}) and the lowest in Bhattian (3.839×10^{-3}). All village LCR values fall within the US-EPA acceptable carcinogenic risk range of 1×10^{-6} to 1×10^{-4}. ICRP Publication 115 [44] reports that each 100 Bq·m^{-3} increase in radon concentration raises lung cancer risk by 16% a relationship that amplifies considerably in smokers. Given that adult male smoking prevalence in Pakistan is around 45.5% [45], targeted public health messaging combining radon awareness with smoking cessation would be the most effective risk-reduction strategy to mitigate lung cancer cases for this population. Radon gas measurements also help in a better prediction of seismic events and they should be monitored continually in the seismically active regions of Pakistan [25].

3.5. Comparison with Worldwide Studies

In this section, **Table 4** compares the study's average indoor radon concentration (43.75 ± 31.04 Bq·m^{-3}) to data from different countries. Numerous countries show average indoor radon levels lower than those measured in Kotli Sattian. In Haryana, India, 91 dwellings had an average of 22 Bq·m^{-3}, with values ranging from 9 to 94 Bq·m^{-3}. Libya had an average of 29 Bq·m^{-3} (range from 5 to 54 Bq·m^{-3}), while Saudi Arabia had an average of 31 Bq·m^{-3}. The data from arid and semi-arid geological environments with sandy and limestone substrates show slightly lower radon emanation compared to the folded metamorphic and sedimentary phases beneath Kotli Sattian. The average indoor radon concentration in the United States is around 50 Bq·m^{-3}, which is consistent with the findings of this study. Numerous investigations show mean radon concentrations that are consistent with the current findings. A preliminary survey of 800 houses in Beijing, China, revealed a mean of 42 Bq·m^{-3} with a range of 12 - 119 Bq·m^{-3}, which closely matched our results in both mean and range. Western Iran (Aleshtar) had an average of 43 Bq·m^{-3}, while Kilis, Osmaniye, and Antakya, Türkiye, reported averages ranging from 40 to 51 Bq·m^{-3}. Several analogous mountainous and seismically active places have elevated indoor radon levels. The Kathmandu Valley in Nepal, a comparable sub-Himalayan seismic zone, had an average of 67 Bq m^{-3} across 50 households, with values reaching 135 Bq·m^{-3}, while earthquake-affected Gorkha had averages as high as 104 Bq·m^{-3}. Iraq had an average of 63 Bq·m^{-3}. Bingöl Province, Türkiye, located on the Anatolian fault system, recorded a mean of 103 Bq·m^{-3}, more than doubling our values, which is consistent with the region's high seismicity and uranium-rich basement geology. Indonesia (Bangka Island) recorded a mean of 56 Bq·m^{-3}, whereas Bangladesh (Dhaka) reported 63 Bq·m^{-3}. The higher values in Nepal and eastern Türkiye when compared to Kotli Sattian are instructive; both places are sub-Himalayan or Alpide belt fault zones with similar tectonic properties. This suggests that local geological makeup, rather than tectonic context, is the primary factor affecting Kotli Sattian's unusually low concentrations. Kotli Sattian falls within the global average for indoor radon levels in residential areas, with a mean concentration of 43.75 Bq·m^{-3} and a range of 13.77 - 135.76 Bq·m^{-3}. This international comparison confirms that radon levels in Kotli Sattian provide no significant public health concern when compared to global standards; however, continuing monitoring is recommended due to the area's seismic activity and aged housing structures.

Table 4. Comparison of indoor radon concentration in Kotli Sattian with worldwide studies.

Country/Region	No. of Dwellings	Mean Radon (Bq·m^{-3})	Range (Bq·m^{-3})	Ref.	vs. Present Study
India (Haryana)	91	22	9 - 94	[46]	Lower
Libya	56	29	5 - 54	[47]	Lower
USA (national)	-	50	-	[48]	Comparable
Saudi Arabia	50	31	18 - 41	[49]	Lower
China (Beijing)	800	42	12 - 119	[50]	Comparable
Western Iran	56	43	1 - 197	[51]	Comparable
Türkiye (Kilis)	204	47	-	[52]	Comparable
Nepal (Kathmandu)	50	67	11 - 135	[53]	Higher
Iraq	50	63	20 - 114	[54]	Higher
Indonesia (Bangka)	94	56	-	[55]	Higher
Bangladesh (Dhaka)	-	63	11 - 360	[56]	Higher
Türkiye (Bingöl)	77	103	43 - 348	[57]	Higher
Pakistan (Present Work)	**25**	**43.75**	**13.77 - 135.76**	-	-

4. Strengths, Limitations and Recommendations

Strengths: This work offers the first baseline evaluation of indoor radon levels in Kotli Sattian, addressing a significant deficiency in the environmental radioactivity literature for the sub-Himalayan area of northern Punjab, Pakistan. The employment of CR-39 solid-state nuclear track detectors a proven and globally acknowledged passive technique facilitated economical and dependable integrated measurements throughout five villages and two types of dwelling construction simultaneously. The health risk assessment was broadened to encompass Excess Lifetime Cancer Risk (ELCR) and radon-specific Lung Cancer Risk (LCR), in addition to GIS-based spatial interpolation, thereby offering a thorough radiological and public health characterization of the study area. **Limitations:** The primary limitation is that all measurements were taken within a single 60-day period, and indoor radon concentrations are recognized to be 1.5 - 2 times greater in winter than in summer due to diminished ventilation and heightened pressure differentials; thus, the reported values may underrepresent the actual annual mean. The study utilized only five houses per village, which, due to the significant intra-village coefficients of variation observed (34% - 95%), restricts the statistical representativeness of the village-level means.

Recommendation: Subsequent research should implement detectors during all four seasons or for a complete 12-month duration, with at least 10 residences per each village, to produce statistically significant yearly average concentrations in accordance with WHO criteria.

5. Conclusion

This study provides the first baseline assessment of indoor radon concentrations in 25 dwellings across five villages of Kotli Sattian, a seismically active sub-Himalayan region in northern Punjab, Pakistan. CR-39 solid-state nuclear track detectors were deployed for 60 days at head height in each dwelling, covering five room types and two construction categories. The overall mean indoor radon concentration was determined to be 43.75 ± 31.04 Bq/m^3, with individual house values ranging from 13.77 Bq/m^3 (H23, Chaffar) to 135.76 Bq/m^3 (H10, Thoon). At the village level, the highest mean radon concentration was recorded in Chaffar (51.85 ± 40.53 Bq/m^3) and the lowest in Bhattian (33.10 ± 11.29 Bq/m^3). All recorded values fall below the US-EPA action level of 150 Bq/m^3 and the ICRP reference level of 300 Bq/m^3; only one house (H10, Thoon) exceeded the WHO reference level of 100 - 300 Bq/m^3. Newly constructed houses in Bhattian, Paija, and Thoon, built from concrete, bricks, and cement, recorded a higher mean radon concentration (49.44 Bq/m^3) than older mud and wood dwellings in Kamra and Chaffar (35.42 Bq/m^3), consistent with the higher radium content of modern construction materials. Three outlier houses in Chaffar and Kamra (H5, H22, H25) exhibited disproportionately elevated concentrations, attributed to the region's active fault system facilitating soil-gas radon migration through unrepaired structural cracks, an effect compounded by limited household resources for maintenance. The mean annual effective dose across all villages was calculated to be 0.11 mSv·y^{-1} well below the ICRP, WHO, and US-EPA public exposure limit of 1 mSv·y^{-1}. The overall Excess Lifetime Cancer Risk (ELCR) of 0.3703×10^{-3} falls within the ICRP acceptable range of 0.29×10^{-3} to 1.45×10^{-3}, and the radon-specific Lung Cancer Risk (LCR) of 5.075×10^{-3} is within internationally accepted limits, collectively confirming that the population of Kotli Sattian does not face an elevated radiological health burden from indoor radon under current conditions. Nonetheless, year-round monitoring, expanded village coverage, fault-proximity spatial analysis, and targeted remediation of the three outlier dwellings are recommended as priorities for future work.

Data Availability

The datasets obtained and analysed during the current study are available from the corresponding author (M. Anjum; mav.mavia14@gmail.com) on reasonable request.

Ethics Approval and Consent to Participate

Informed verbal consent was obtained from the occupants of all 25 dwellings prior to dosimeter installation. No biological samples were collected, and no ethical approval was required for this environmental measurement study.

Acknowledgements

We would like to thank University of Idaho department of Physics for providing access to the literature online.

Author Contributions

M. Anjum conceptualised and designed the study, led the experimental analysis, performed all dosimetric calculations and health risk assessments (ELCR and LCR), wrote the original draft of the manuscript, and managed the overall project coordination. **A. Hashir**, **S. Jamil**, and **A. Khalid** performed field sample collection, CR-39 detector deployment and retrieval, chemical etching, and track counting in the laboratory. **M. A. M. Azmin**, **M. Bashir and A. Abbas** contributed to software analysis, GIS mapping and figure preparation, and participated in reviewing and editing the manuscript. **H. Younis** and **M. Nadeem** supervised the research, provided laboratory resources and infrastructure, and reviewed and edited the manuscript. All authors have read and approved the final manuscript.

Conflicts of Interest

The authors declare that they have no competing interests.

References

[1] Anjum, M., Siddique, N., Younis, H., Faiz, Y., Shafique, M.A., Mahnoor, A., *et al.* (2024) Heavy Metals and Radionuclides in Islamabad's Industrial Area: A Comprehensive Analysis of Soil and Water Pollution, Source Apportionment and Health Effects Using Statistical and Geospatial Tools. *Journal of Trace Elements and Minerals*, **8**, Article 100127. https://doi.org/10.1016/j.jtemin.2024.100127

[2] Kapdan, E. and Altinsoy, N. (2012) A Comparative Study of Indoor Radon Concentrations between Dwellings and Schools. *Radiation Physics and Chemistry*, **81**, 383-386. https://doi.org/10.1016/j.radphyschem.2011.12.032

[3] Sajid, A., Anjum, M., Younis, H., Salouci, M., Mehboob, K. and Haj Ismail, A. (2024) Assessment of Radon Concentration and Health Hazards in Natural Spring Water of a Sub-Himalayan District. *Atmosphere*, **15**, Article 940.

https://doi.org/10.3390/atmos15080940

[4] Santos-Francés, F., Gil Pacheco, E., Martínez-Graña, A., Alonso Rojo, P., Ávila Zarza, C. and García Sánchez, A. (2018) Concentration of Uranium in the Soils of the West of Spain. *Environmental Pollution*, **236**, 1-11. https://doi.org/10.1016/j.envpol.2018.01.038

[5] Anjum, M., Siddique, N., Younis, H., Faiz, Y., Shafique, M.A., *et al.* (2024) Evaluating Heavy Metal Contamination and Radiological Effects in Soil Samples from Murree, Pakistan. *Environmental Earth Sciences*, **83**, Article No. 361. https://doi.org/10.1007/s12665-024-11673-4

[6] National Research Council, Committee on Life Sciences, Board on Radiation Effects Research and Committee on Health Risks of Exposure to Radon (BEIR VI) (1999) Health Effects of Exposure to Radon: BEIR VI. National Academies Press, Washington DC.

[7] Mansour, H.H., Khdar, S., Abdulla, H.Y., Muhamad, N.Q., Othman, M.M. and Qader, S. (2005) Measurement of Indoor Radon Levels in Erbil Capital by Using Solid State Nuclear Track Detectors. *Radiation Measurements*, **40**, 544-547. https://doi.org/10.1016/j.radmeas.2005.06.033

[8] Barkat, A., Ali, A., Hayat, U., Crowley, Q.G., Rehman, K., Siddique, N., *et al.* (2018) Time Series Analysis of Soil Radon in Northern Pakistan: Implications for Earthquake Forecasting. *Applied Geochemistry*, **97**, 197-208. https://doi.org/10.1016/j.apgeochem.2018.08.016

[9] Pawel, D.J. and Puskin, J.S. (2004) The U.S. Environmental Protection Agency's Assessment of Risks from Indoor Radon. *Health Physics*, **87**, 68-74. https://doi.org/10.1097/00004032-200407000-00008

[10] World Health Organization (2023) Radon. https://www.who.int/news-room/fact-sheets/detail/radon-and-health

[11] Ting, D.S. (2010) WHO Handbook on Indoor Radon: A Public Health Perspective. *International Journal of Environmental Studies*, **67**, 100-102. https://doi.org/10.1080/00207230903556771

[12] Lecomte, J.F., Solomon, S., Takala, J., Jung, T., Strand, P., Murith, C., *et al.* (2014) ICRP Publication 126: Radiological Protection against Radon Exposure. *Annals of the ICRP*, **43**, 5-73. https://doi.org/10.1177/0146645314542212

[13] Feroze, R., Younis, H., Ahmad, M.A., Khan, M.A., Rehman, S.U., Jagnandan, S., *et al.* (2025) Dosimetric Analysis of True Beam Linear Accelerators and Assessment of Dosimetry of Photon Beams for Various Treatment Parameters. *The European Physical Journal Plus*, **140**, Article No. 155. https://doi.org/10.1140/epjp/s13360-025-06091-9

[14] Azmin, M.A.M., Younis, H., Anjum, M., Abbas, A. and Tariq, I. (2026) Radiological and Environmental Assessment of Radon Emanation from Soil and Water in the Islamabad Region of Northern Pakistan. *Discover Soil*, **3**, Article No. 83. https://doi.org/10.1007/s44378-026-00242-9

[15] Appleton, J.D. (2013) Radon in Air and Water. In: *Essentials of Medical Geology*, Springer Netherlands, 239-277. https://doi.org/10.1007/978-94-007-4375-5_11

[16] Charles, M. (2001) UNSCEAR Report 2000: Sources and Effects of Ionizing Radiation. *Journal of Radiological Protection*, **21**, 83-85. https://doi.org/10.1088/0952-4746/21/1/609

[17] United Nations Scientific Committee on the Effects of Atomic Radiation (n.d.) UNSCEAR 2000 Report Volume I. https://www.unscear.org/unscear/en/publications/2000_1.html

[18] World Health Organization (2009) WHO Handbook on Indoor Radon: A Public

Health Perspective. World Health Organization, Geneva. https://www.who.int/publications/i/item/9789241547673

[19] Akerblom, G. and Wilson, C. (1982) Radon—Geological Aspects of an Environmental Problem: Environmental Radon Investigation in Sweden—Regional Environmental Documentation of Natural Radiation in Sweden. Sveriges Geologiska Undersoekning, Uppsala. https://www.osti.gov/biblio/6493816

[20] Weblinx (2014) 7 Ways Radon Enters Your Home. Trinity Electrical Services, Inc. https://www.tesyes.com/blog/radon-enters-home/

[21] Henschel, D.B. and Scott, A.G. (1991) Causes of Elevated Post-Mitigation Radon Concentrations in Basement Houses Having Extremely High Pre-Mitigation Levels. https://www.aivc.org/sites/default/files/airbase_5476.pdf

[22] Espinosa, G., Golzarri, J.I., Chavarria, A. and Castaño, V.M. (2013) Indoor Radon Measurement via Nuclear Track Methodology: A Comparative Study. *Radiation Measurements*, **50**, 127-129. https://doi.org/10.1016/j.radmeas.2012.09.010

[23] Amin, R.M. (2014) Evaluation of Radon Gas Concentration in the Drinking Water and Dwellings of South-West Libya, Using CR-39 Detectors. *International Journal of Environmental Sciences*, **4**, 484-490.

[24] Anjum, M., Siddique, N., Younis, H., Faiz, Y., Shafique, M.A., *et al*. (2024) Chemometric Evaluation, Source Apportionment, and Health Risk Analysis of Natural Spring Water in Murree, Outer Himalayas. *Journal of Trace Elements and Minerals*, **10**, Article 100195. https://doi.org/10.1016/j.jtemin.2024.100195

[25] Younis, H., Afzal, M.W., Anjum, M., Hussain, J., Mehboob, K. and Ajaz, M. (2024) Quantification of Natural Radioactivity, Radon Levels, and Radiological Health Hazards in Soil from Seismic Fault Zones. *The European Physical Journal Plus*, **139**, Article No. 1017. https://doi.org/10.1140/epjp/s13360-024-05823-7

[26] Gogoi, P.P., Phukan, S. and Barooah, D. (2025) Radiological Risk Assessment of Indoor 222Rn and 220Rn Exposure in the Seismically Active Kopili Fault Zone on the Eastern Wedge of the Shillong Plateau, India. *Applied Radiation and Isotopes*, **225**, Article 112104. https://doi.org/10.1016/j.apradiso.2025.112104

[27] Bulut, H.A. and Şahin, R. (2024) Radon, Concrete, Buildings and Human Health—A Review Study. *Buildings*, **14**, Article 510. https://doi.org/10.3390/buildings14020510

[28] Chen, Z., Li, Y., Liu, Z., Wang, J., Zhou, X. and Du, J. (2018) Radon Emission from Soil Gases in the Active Fault Zones in the Capital of China and Its Environmental Effects. *Scientific Reports*, **8**, Article No. 16772. https://doi.org/10.1038/s41598-018-35262-1

[29] Abbas, S.Q., Khan, J., Riaz, M.T., Rafique, M., Zaman, A. and Khan, S. (2023) Radon Concentration in Spring Water as an Indicator of Seismic Activity: A Case Study of the Muzaffarabad Fault in Pakistan. *Environmental Monitoring and Assessment*, **196**, Article No. 41. https://doi.org/10.1007/s10661-023-12235-0

[30] Khan, F., Khattak, S.A., Wazir, Z. and Waqas, M. (2021) Spatial Distribution of Radon Concentrations in Balakot-Bagh (B-B) Fault Line and Adjoining Areas, Lesser Himalayas, North Pakistan. *Environmental Earth Sciences*, **80**, Article No. 291. https://doi.org/10.1007/s12665-021-09569-8

[31] Rathebe, P.C., Mphaga, K.V. and Masekameni, D.M. (2025) Climate Change and Environmental Radioactivity: A Review of Studies on Climate Conditions in Variation on Indoor Radon Concentrations. *Environmental Monitoring and Assessment*, **197**, Article No. 446. https://doi.org/10.1007/s10661-025-13889-8

[32] Iqbal, A., Baig, M.S., Akram, M. and Qureshi, A.A. (2012) Indoor Radon Concentra-

tion Levels, Gamma Dose Rates and Impact of Geology—A Case Study in Kotli, State of Azad Jammu and Kashmir, Sub-Himalayas, in Pakistan. *Radioprotection*, **47**, 253-270. https://doi.org/10.1051/radiopro/2012005

[33] Liu, Y., Fu, C., Li, Y., Xu, W., Huang, Z. and Xu, Y. (2025) Uncovering Hidden Dangers in Urban Housing: Sources of Indoor Radon and Associated Health Risks. *Journal of Environmental Management*, **387**, Article 125899. https://doi.org/10.1016/j.jenvman.2025.125899

[34] Borgoni, R., Tritto, V., Bigliotto, C. and De Bartolo, D. (2011) A Geostatistical Approach to Assess the Spatial Association between Indoor Radon Concentration, Geological Features and Building Characteristics: The Case of Lombardy, Northern Italy. *International Journal of Environmental Research and Public Health*, **8**, 1420-1440. https://doi.org/10.3390/ijerph8051420

[35] Nunes, L.J.R., Curado, A. and Lopes, S.I. (2023) The Relationship between Radon and Geology: Sources, Transport and Indoor Accumulation. *Applied Sciences*, **13**, Article 7460. https://doi.org/10.3390/app13137460

[36] Turk, B.H., Prill, R.J., Grimsrud, D.T., Moed, B.A. and Sextro, R.G. (1990) Characterizing the Occurrence, Sources, and Variability of Radon in Pacific Northwest Homes. *Journal of the Air & Waste Management Association*, **40**, 498-506. https://doi.org/10.1080/10473289.1990.10466705

[37] Elewee, A.A. and Aswood, M.S. (2022) Estimation of Indoor Radon Concentration in Some Houses in Al-Shatra District, Dhi-Qar Governorate, Iraq. *Nature Environment and Pollution Technology*, **21**, 1747-1752. https://doi.org/10.46488/nept.2022.v21i04.029

[38] Ali, N., Khan, E.U., Akhter, P., Khan, F. and Waheed, A. (2010) Estimation of Mean Annual Effective Dose through Radon Concentration in the Water and Indoor Air of Islamabad and Murree. *Radiation Protection Dosimetry*, **141**, 183-191. https://doi.org/10.1093/rpd/ncq160

[39] Ur-Rahman, S., Rafique, M., Matiullah, and Anwar, J. (2009) Indoor Radon Concentrations and Assessment of Doses in Four Districts of the Punjab Province—Pakistan. *Journal of Radiation Research*, **50**, 529-535. https://doi.org/10.1269/jrr.08116

[40] Khan, F., Ali, N., Khan, E.U., Khattak, N.U., Raja, I.A., Baloch, M.A., *et al.* (2012) Study of Indoor Radon Concentrations and Associated Health Risks in the Five Districts of Hazara Division, Pakistan. *Journal of Environmental Monitoring*, **14**, 3015-3023. https://doi.org/10.1039/c2em30445g

[41] Amir, M.W., Malik, A.H., Raza, Z. and Saad, M. (2022) Time Series Modeling and Prediction of Life Expectancy Rate at Birth in Pakistan. https://www.researchgate.net/profile/Muhammad-Saad-Khan-8/publication/393136969

[42] International Commission on Radiological Protection (2007) Preface, Executive Summary and Glossary. *Annals of the ICRP*, **37**, 9-34.

[43] Kang, J.K., Seo, S. and Jin, Y.W. (2019) Health Effects of Radon Exposure. *Yonsei Medical Journal*, **60**, 597-603. https://doi.org/10.3349/ymj.2019.60.7.597

[44] Clement, C.H., Tirmarche, M., Harrison, J.D., Laurier, D., Paquet, F., Blanchardon, E., *et al.* (2010) Lung Cancer Risk from Radon and Progeny and Statement on Radon. *Annals of the ICRP*, **40**, 1-64. https://doi.org/10.1016/j.icrp.2011.08.011

[45] Datta, B.K., Husain, M.J. and Nargis, N. (2019) An Intertemporal Analysis of Post-FCTC Era Household Tobacco Consumption in Pakistan. *International Journal of Environmental Research and Public Health*, **16**, Article 2532. https://doi.org/10.3390/ijerph16142532

[46] Panghal, A., Kumar, A. and Kumar, S. (2019) Seasonal Variation of Indoor Radon–Thoron Levels in Dwellings of Four Districts of Haryana, India. *Science and Technology for the Built Environment*, **25**, 103-111. https://doi.org/10.1080/23744731.2018.1500395

[47] Taye, A.E. and Chandravanshi, B.S. (2023) Health and Ecological Risk Assessment of Potentially Toxic Metals in Road Dust at Lalibela and Sekota Towns, Ethiopia. *Environmental Monitoring and Assessment*, **195**, Article No. 765. https://doi.org/10.1007/s10661-023-11406-3

[48] US Environmental Protection Agency (2019) What Is EPA's Action Level for Radon and What Does It Mean. US EPA, Washington DC. https://www.epa.gov/radon/what-epas-action-level-radon-and-what-does-it-mean

[49] Amin, R.M. (2015) Assessment of Concentration and Exposure Doses Due to Radon by Using CR-39 Plastic Track Detectors in the Dwellings of Saudi Arabia. *Advances in Applied Science Research*, **6**, 42-48. https://www.primescholars.com/articles/assessment-of-concentration-and-exposure-doses-due-to-radon-by-using-cr39plastic-track-detectors-in-the-dwellings-of-saudi-arabia.pdf

[50] Wang, H., Zhang, L., Gao, P. and Guo, Q. (2022) A Pilot Survey on Indoor Radon Concentration in Beijing. *Radiation Medicine and Protection*, **3**, 22-25. https://doi.org/10.1016/j.radmp.2022.01.003

[51] Hassanvand, H., Birjandi, M., Amiri, A., Hassanvand, M.S. and Kamarehie, B. (2019) Investigation of Indoor Radon Concentration in Dwellings of Aleshtar (Western Part of Iran) and Estimation of the Annual Effective Dose from Exposure to Radon. *International Journal of Radiation Research*, **17**, 659-666.

[52] Can, B., Canbazoğlu, C., Albayrak, N., Çelebi, N. and Doğru, M. (2011) Measurements of Indoor Radon Concentration Levels in Kilis, Osmaniye and Antakya, Turkey during Spring Season. *Journal of Radioanalytical and Nuclear Chemistry*, **292**, 1059-1063. https://doi.org/10.1007/s10967-011-1559-z

[53] Rijal, B., Silwal, N.S., Chaudhary, G., Shrestha, P. and Shah, B.R. (2021) Radon Study around Earthquake Affected Areas of Nepal. *Bibechana*, **18**, 61-67. https://doi.org/10.3126/bibechana.v18i2.29840

[54] Mir, A.A., Celebi, F.V., Alsolai, H., Qureshi, S.A., Rafique, M., Alzahrani, J.S., *et al.* (2022) Anomalies Prediction in Radon Time Series for Earthquake Likelihood Using Machine Learning-Based Ensemble Model. *IEEE Access*, **10**, 37984-37999. https://doi.org/10.1109/access.2022.3163291

[55] Pradana, R., Nugraha, E.D., Omori, Y., Shilfa, S.N., Winarni, I.D., Wahyudi, W., *et al.* (2024) Public Exposure from Inhalation of Radon and Thoron around the Tin Mine and Smelter Areas in Bangka, Indonesia. *Scientific Reports*, **14**, Article No. 30731. https://doi.org/10.1038/s41598-024-80443-w

[56] Pervin, S., Yeasmin, S., Khandaker, M.U. and Begum, A. (2022) Radon Concentrations in Indoor and Outdoor Environments of Atomic Energy Centre Dhaka, Bangladesh, and Concomitant Health Hazards. *Frontiers in Nuclear Engineering*, **1**, Article 901818. https://doi.org/10.3389/fnuen.2022.901818

[57] Koc, P., Ekinci, N., Cinan, E. and Kavaz, E. (2018) Determination of Radon Concentration by Using CR-39 Plastic Track Detectors in Dwellings of Bingöl and Mus Provinces of Turkey. *Asian Journal of Chemistry*, **30**, 226-230. https://doi.org/10.14233/ajchem.2018.21094